IMPROVED TWO-DIMENSIONAL-KINETICS

COMPUTER PROGRAM

NAS8-35931

Second Quarterly Progress Report

1 April 1984 through 30 June 1984

Prepared by: Gary R. Nickerson
                Software and Engineering Associates, Inc.
                1560 Brookhollow Drive, Suite 203
                Santa Ana, California 92705

IMPROVED TWO-DIMENSIONAL-KINETICS COMPUTER PROGRAM

1.0 BACKGROUND

Future Orbit Transfer Vehicles (OTV) presently under consideration need rocket engines delivering a high specific impulse. This high performance can be obtained with large area ratio thrust chambers using oxygen with either hydrogen or hydrocarbon fuels. In the projected nozzles the combustion products are expanded to low pressure and temperature levels at high Mach-number flow, a domain which has not been experienced with existing rocket engines.

Some modifications have recently been incorporated in the Two-Dimensional-Kinetics (TDK) computer program, such as: Condensed phase flow simulation, treatment of shock waves induced by the wall curvature, and the coupling of the TDK code with the Boundry Layer Module (BLM) for an improved thrust chamber specific impulse prediction.

Recent boundary layer calculations for large area ratio nozzles have revealed that the boundary layer becomes very thick in the region of high Mach-numbers. This result is quite different from rocket engines built up to now and requires an examination of the existing thrust loss calculation method due to the viscous effects adjacent to the wall. Furthermore, the knowledge of the Knudsen-number is desirable which differentiates between continuum, slip and free molecular flow, and thereby identified when the analysis, presently based on Newtonian fluid flow, becomes questionable or invalid.

In order to obtain highly accurate performance predictions, the best supporting data for equilibrium and finite rate chemistry must be prepared. Furthermore, the large area ratio nozzles require many more calculation steps to cover the complete nozzle flow field. This increases computation time significantly and favors an error accumulation which should be reduced as much as possible. Another point of importance connected with the OTV is the existence of ionized combustion products which permits vehicle tracing or interferes with the transfer of communication or command signals.

The current effort of shock wave modeling induced by the curvature of the wall should be expanded to permit the shock simulation caused by wall contour discontinuities. Also the Mach shock existence in the center of the flow field interacting with other shocks as well as the analytical treatment of multiple shock waves may significantly affect the interior nozzle flow and associated performance and need to be simulated.

2.0 OBJECTIVE

The objective of this effort is to increase the analytical capability of the existing TDK/BLM computer program for performance of OTV thrust chambers. Areas which need further examination and improvement are the thick boundary layer inviscid core flow interaction and the related thrust loss calculation. To warrant highly accurate results the provision of the best available program input data is mandatory as well as the use of sophisticated modeling techniques to reduce computation time with advanced error control criteria. The simulation of wall shocks, Mach-shocks in addition to shocks induced by large concave wall curvature is essential since this interaction with each other produces flow field changes which in turn affect the nozzle performance.

3.0 WORK PERFORMED DURING THE REPORTING PERIOD

The program plan for this work is presented in Figure 1. Progress in each of the work tasks is presented in the sub-paragraphs 3.1 through 3.5. One trip was also taken during the reporting period.

Mr. Nickerson and Dr. Dang spent Wednesday, 23 May 1984, at NASA MSFC discussing the status of the contract with Mr. Gross and Mr. Krebsback. The 24th of May was spent in attendance at the Performance Standardization Subcommittee Liquid Panel Meeting held at NASA MSFC where Mr. Nickerson gave a technical presentation on the work being performed under this contract.
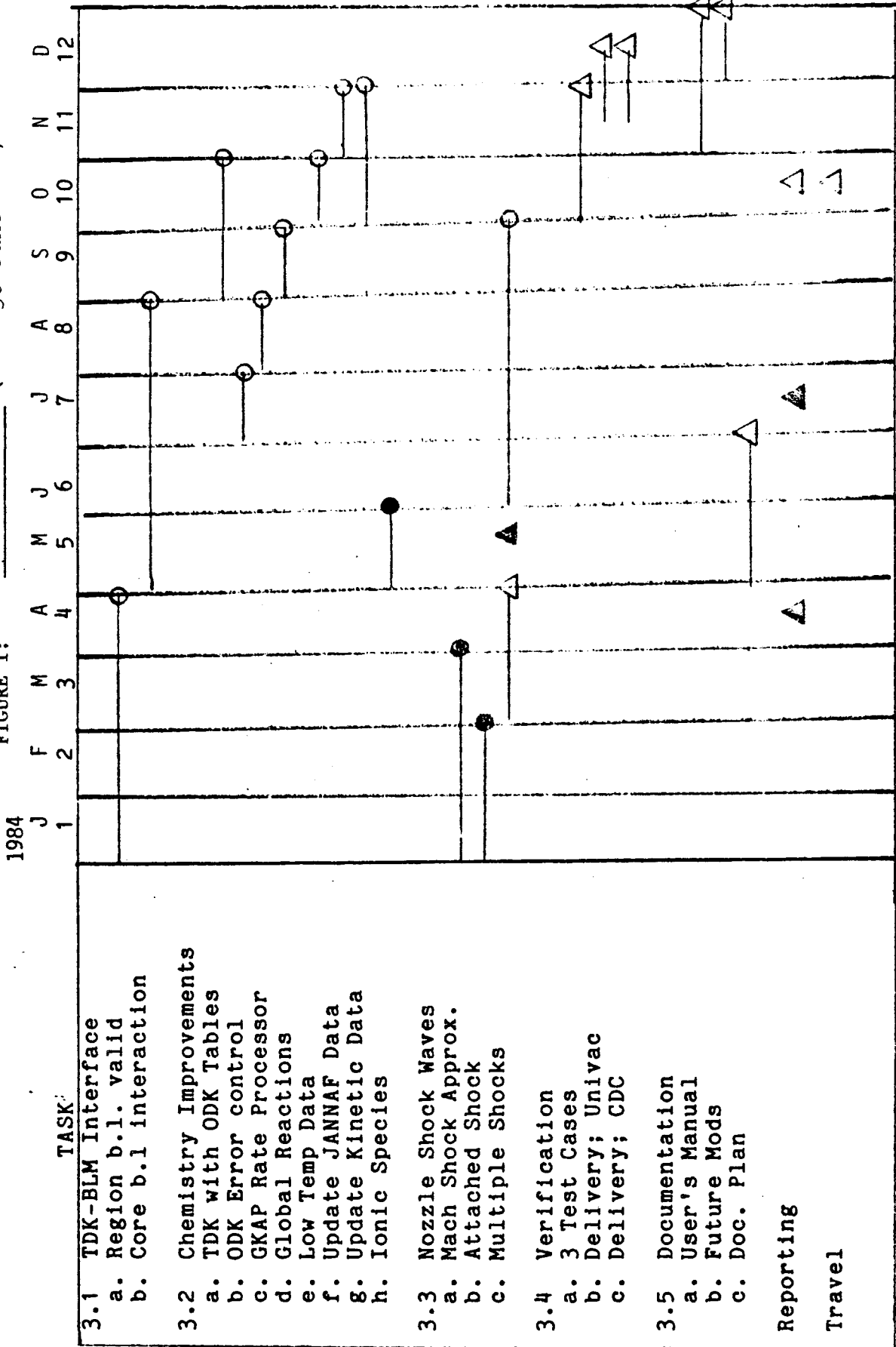
3.1 TDK-BLM INTERFACE

Work has continued on this task throughout the reporting period. A report draft has been prepared on this subject for SEA by Dr. Waldman and is attached.

3.2 CHEMISTRY IMPROVEMENTS

The ODK and TDK modules have been modified to treat electrons and ionic species. To do this required establishment of a proper linkage of these modules with the ODE module. This task, 3.2h, was requested by the AFRPL. It is particularly useful for obtaining nozzle exit plane properites to be used as starting conditions for exhaust plume calculations. Reference 1 is a good source for reactions and rates for these processes.

Ref. 1: Jensen, P.E. and Jones, G.A., "Reaction Rate Coefficients for Flame Calculations" Combustion and Flame 32, 1-34 (1978)

PROGRAM PLAN (as of 30 June 1984)

FIGURE 1:

1984

TASK	J 1	F 2	M 3	A 4	M 5	J 6	J 7	A 8	S 9	O 10	N 11	D 12
3.1 TDK-BLM Interface												
a. Region b.l. valid												
b. Core b.l interaction												
3.2 Chemistry Improvements												
a. TDK with ODK Tables												
b. ODK Error control												
c. GKAP Rate Processor												
d. Global Reactions												
e. Low Temp Data												
f. Update JANNAF Data												
g. Update Kinetic Data												
h. Ionic Species												
3.3 Nozzle Shock Waves												
a. Mach Shock Approx.												
b. Attached Shock												
c. Multiple Shocks												
3.4 Verification												
a. 3 Test Cases												
b. Delivery; Univac												
c. Delivery; CDC												
3.5 Documentation												
a. User's Manual												
b. Future Mods												
c. Doc. Plan												
Reporting												
Travel												

O scheduled completion
● completion

∠ scheduled delivery
▲ delivery

5

3.3 NOZZLE SHOCK WAVES

The remaining shock wave task to be performed is Task 3.3c, multiple shocks. A detailed approach to this problem has been prepared and was presented to the COR for his approval at MSFC on 28 May, 1984. A copy of the plan, which consists of four tasks, is attached. Tasks 1) and 2) have been done. We are awaiting approval on Tasks 3) and 4).

The SSME was used as a test case in performing Tasks 1) and 2). This is an engine of primary interest to NASA/MSFC. Because of the presents of induced shocks in the nozzle, and also due to the near equilibrium thermodynamic state of the exhaust, the SSME is a very demanding test case. For the right-running characteristics construction method, several numerical refinements were found necessary. These had to do with point insertion and the method for maintaining mass flow balance. The SSME was successfully run and the TDK program modifications were transmitted to NASA.

3.4 A STUDY OF THE BLM WALL HEAT FLUX OPTION

The BLM contains options through which either the wall temperature, or the wall heat flux, can be specified. Since measurements of wall heat flux are sometimes available, the usage of these as a boundary condition for BLM was investigated.

Since an input wall temperature profile will produce an output wall heat flux profile, computer runs were made to determine 1) the consistency, and 2) the sensitivity of the computations. The ASE 400:1 engine was used as a test case. First, zero wall heat flux was requested and the adiabatic wall temperature computed. On a second run, the computed adiabatic wall temperature was input and it was shown that zero heat flux was computed. Next a similar pair of runs were made with a 2000° R wall temperature. This is much cooler than the adiabatic wall. Again, the results checked.

This was followed by a pair of runs using a wall temperature profile provided by NASA, Figure 2, that includes the effects of regen cooling. The resultant wall heat flux is shown in Figure 3. Input of this heat flux then produced the wall temperature profile shown in Figure 4. The predicted temperatures follow those of Figure 1, but show sensitivity because the influence coefficient $\partial T_w / \partial \dot{q}_w$ is evidently large.

To obtain a measure of this sensitivity, the profile for the heat flux out of the wall was decreased by 5% and the case was again run. The result is shown in Figure 5. Wall temperatures were doubled, indicating that $\partial T_w / \partial \dot{q}_w \approx 20$. The shape of the T_w profile is unchanged. The conclusions are that:

1) The T_w and $\dot{q}_w$ computations are consistent.
2) Local $\dot{q}_w$ is governed by local T_w, and visa versa.
3) T_w is highly sensitive to $\dot{q}_w$,
   $\dot{q}_w$ is unsensitive to T_w,

and

4) Except for the adiabatic wall case, $\dot{q}_w = 0$, the input of $\dot{q}_w$ is not very useful. Wall temperature can not be estimated by input of a finite heat flux.
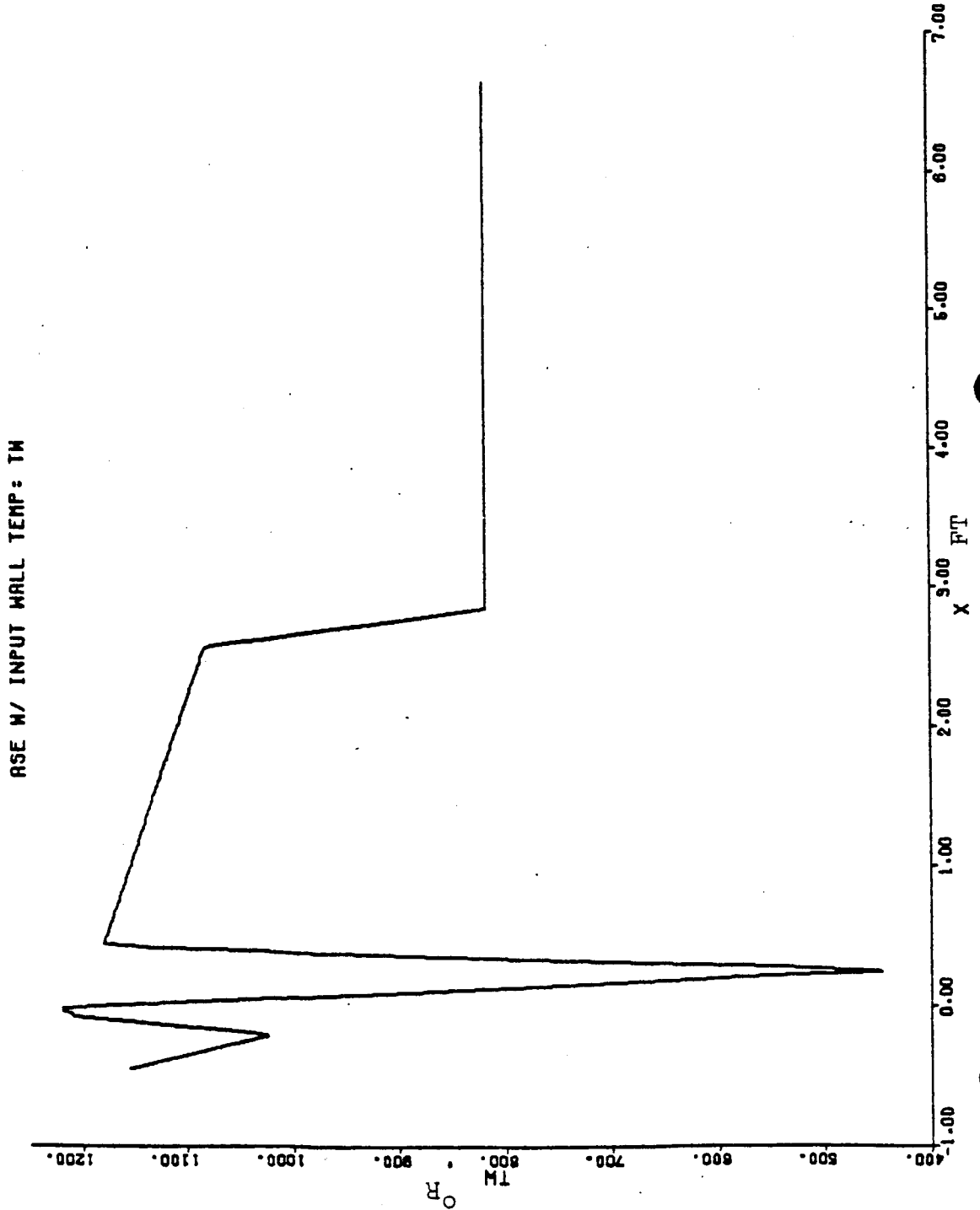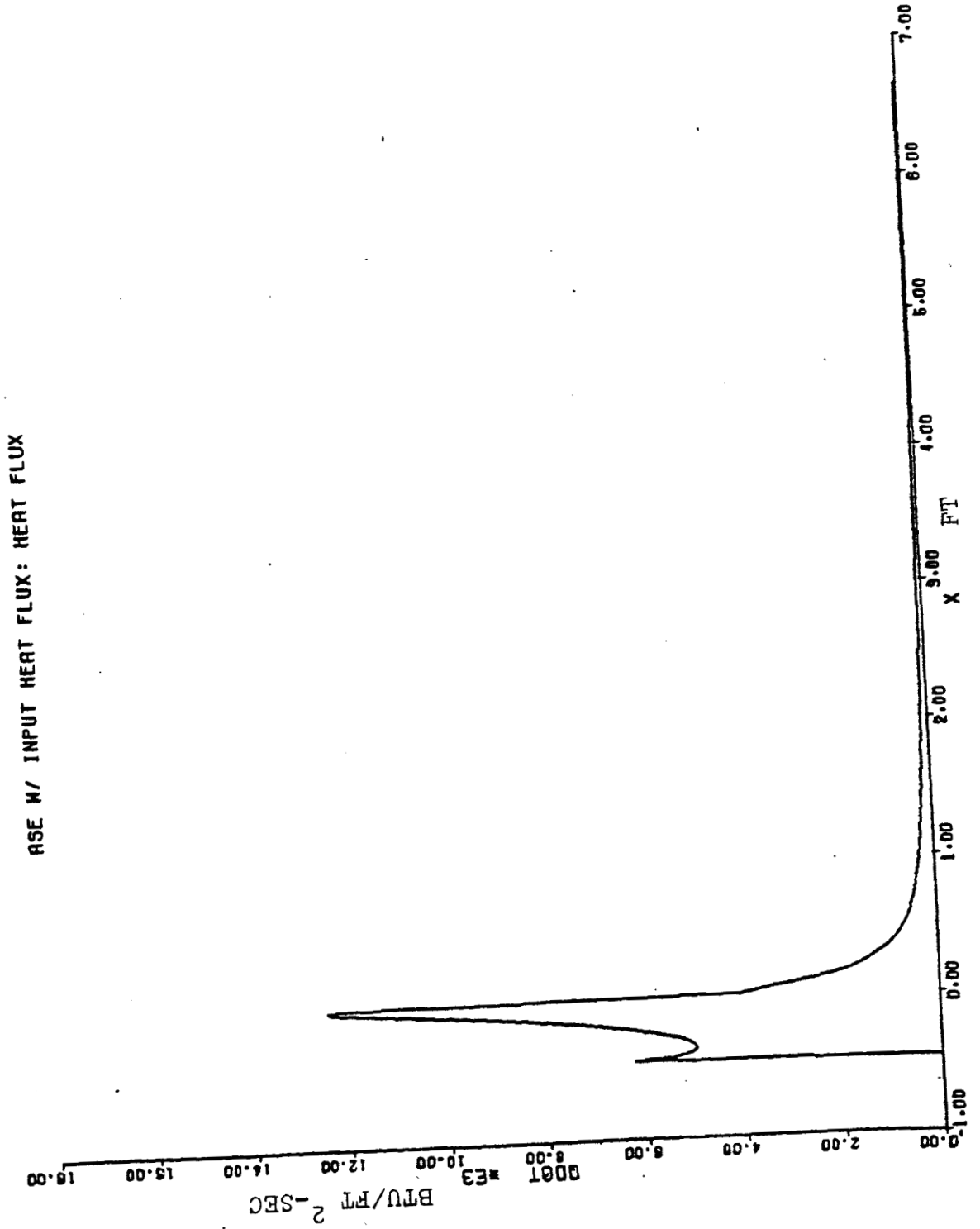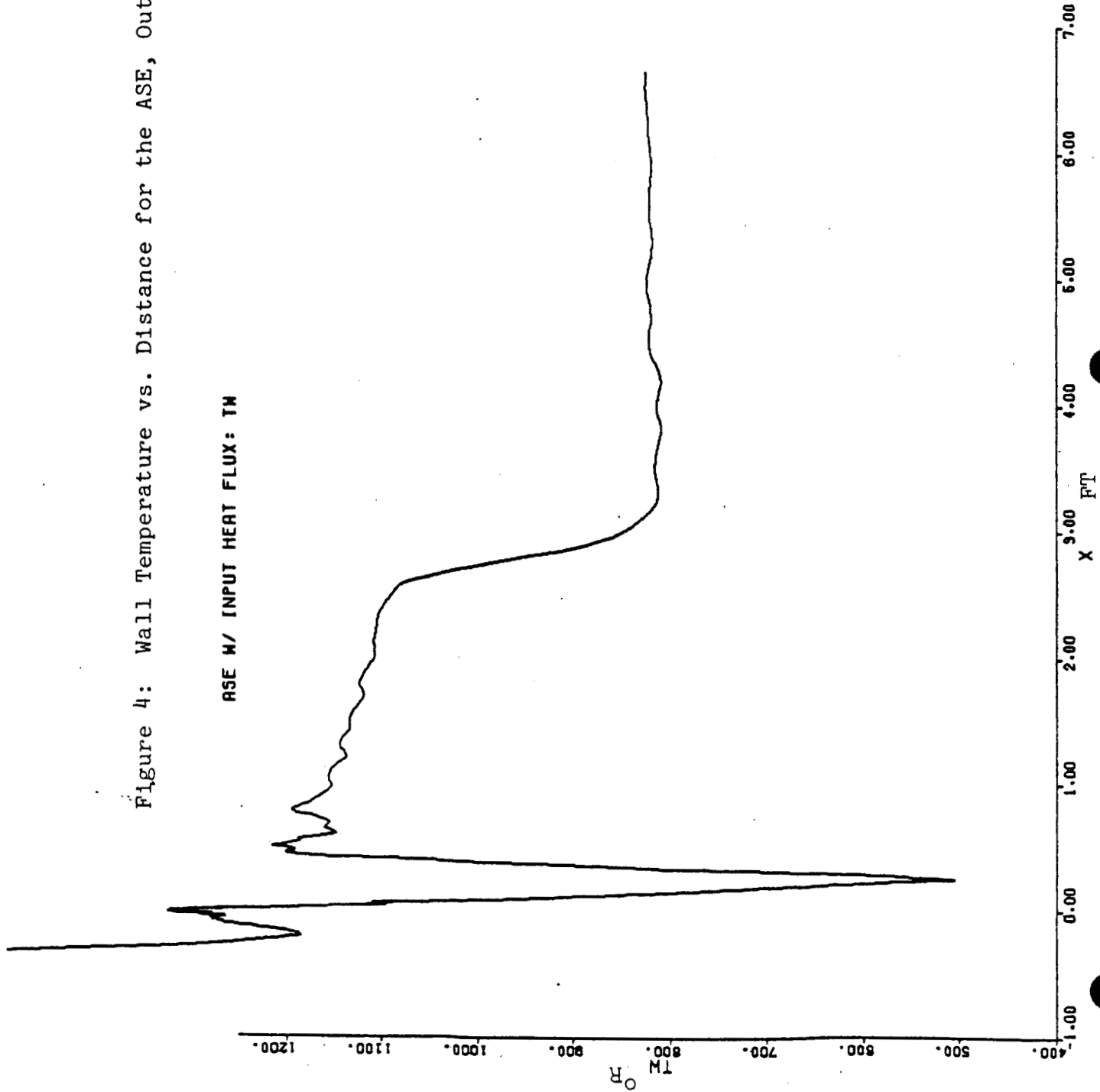
Figure 2: Wall Temperature vs. Distance for the ASE, Input

ASE W/ INPUT WALL TEMP: TW

Figure 3: Wall Heat Flux vs. Distance for the ASE

ASE W/ INPUT HEAT FLUX: HEAT FLUX

6

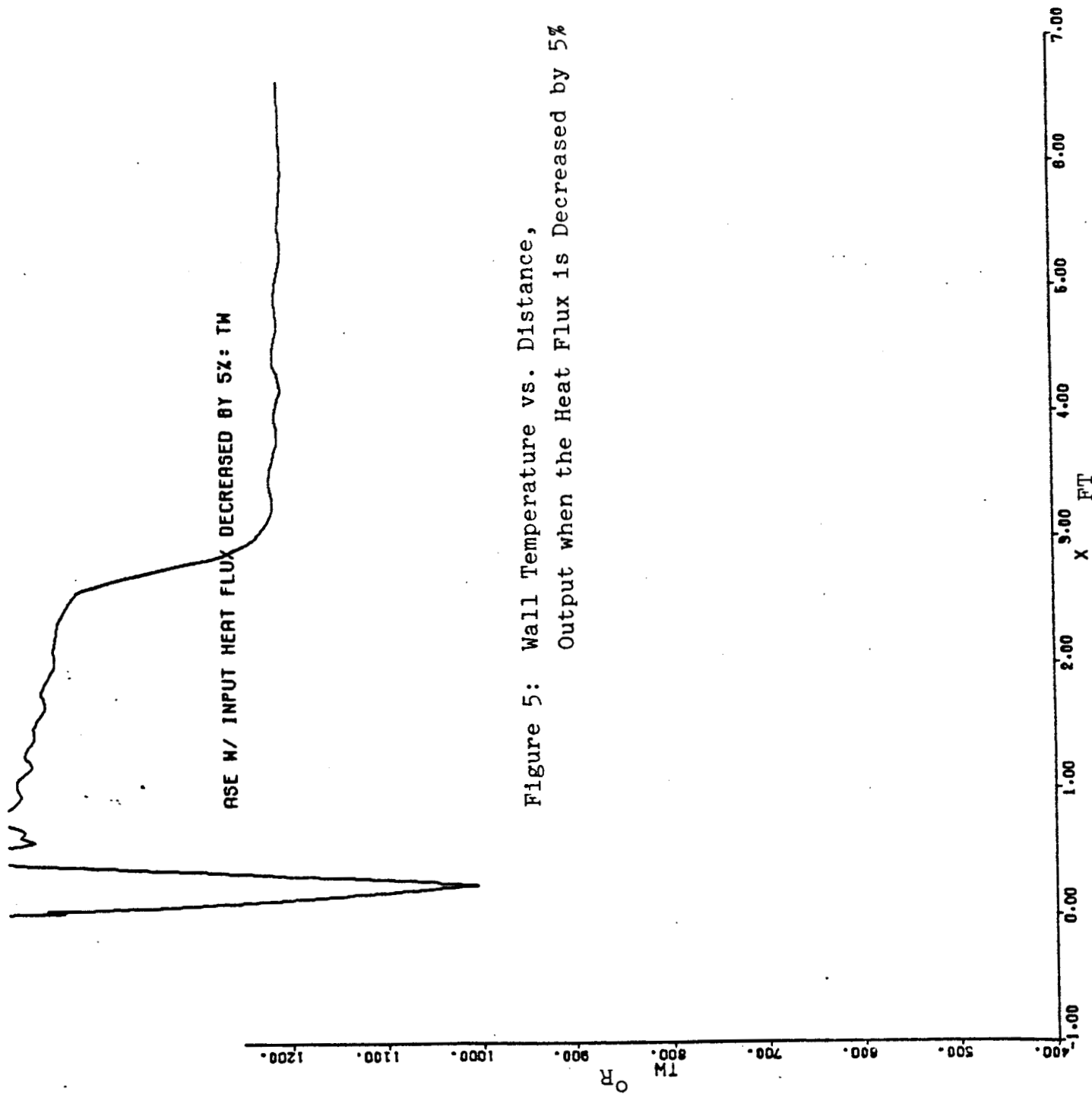Figure 4: Wall Temperature vs. Distance for the ASE, Output

Figure 5: Wall Temperature vs. Distance,
Output when the Heat Flux is Decreased by 5%

11

4.0 WORK PLANNED FOR THE NEXT REPORTING PERIOD

The program plan shown in Figure 1 and during the next quarter are discussed below.

The evaluation of high Mach number and low density effects on the existing boundary layer thrust calculation is to be completed.

The low temperature data task, 3.2e, will be done early, probably during July.

The major task to be worked will be multiple shocks, task 3.3c.

5.0 CURRENT PROBLEM AREAS

The problem areas discussed in the First Quarterly Report have been resolved. Our difficulties with invoicing the work was overcome when a first payment was received at the end of May.

Thus, the first five months of the contract were financed by SEA. This had an adverse effect in that the level of effort was reduced so that the company cash flow could be maintained. At this time the work is about one month behind schedule.

6.0 COST STATUS

As of the end of the reporting period, the cost status of this contract is as follows:

1) Total Cumulative Costs through $ 42,255
   30 June 1984

2) Estimated Cost to Complete $ 76,605

3) Estimated Percentage of Physical $ 35%
   Completion of the Contract

The costs on the contract to date correspond well with the estimated percentage of completion.

OTV Nozzle Design
Thick Turbulent Boundary Layer

18 June 1984

Prepared by
Cye H. Waldman, Ph.D.
Consultant
515 Hermes Avenue
Leucadia, CA 92024
(619) 942-3016

1. Statement of the problem

The JANNAF rocket thrust chamber performance prediction procedure assumes that the nozzle flow field can be separated into a boundary-layer region near the wall in which viscous effects are predominant, and an invisicd core flow containing the bulk of the nozzle mass flow. Basically, the procedure consists of calculating the inviscid flow within the nozzle (the so-called core flow), and then using the flow conditions found adjacent to the wall as representing the inviscid edge of the boundary layer. Conventional methods, such as embodied in the BLIMP-J[1], TBL[2], or BLM[3] computer programs, are then used to compute a displaced wall, i.e., the wall position is displaced by the boundary layer displacement thickness. The process is iterated, if necessary, and a value for the thrust deficit is computed.

However, nozzle designs for OTV applications can be such that most of the nozzle mass flow is confined to a region that is relatively near the wall. This is because of (a) compression of the exhaust gas caused by inward turning of the nozzle contour and (b) area increases significantly near the nozzle wall (r^2-effect). Under these circumstances the boundary layer can grow to such an extent that it interacts with the core flow.

The effect of a thick boundary layer may be significant on the thrust deficit calculation and the JANNAF procedure must be re-examined. There are three effects of potential importance under these conditions which are not accounted for in the classical boundary layer theory: these are the effects of

- transverse curvature

- longitudinal curvature

- fluid stratification

In the following sections these effects will be examined in the light of their impact on the mean flow and eddy-viscosity models. Following that, recommendations will be made regarding improved thrust deficit calculations.

2. Transverse Curvature Effects

Transverse (or lateral) curvature effects become important in axisymmetric flows when the body radius is of the same order as the boundary-layer thickness. The transverse curvature term falls out naturally in the axisymmetic boundary layer equations when transforming from cylindrical to body coordinates (see, for example, **Cebeci & Bradshaw**[4]). The transverse curvature term is included in the BLM program of **Cebeci**[3].

In turbulent flow, the effect of transverse curvature is to alter the mixing length. For external flows it is well-established that mixing length is smaller than its two-dimensional equivalent. Physically, the cylinder has less ability to create turbulence than a plane surface. This has been amply demonstrated in the literature; many experiments have been conducted on the effect of transverse curvature on thick turbulent boundary layers in external flow fields.

A typical study consists of a turbulent boundary layer on the conical tail of a body of revolution. **Patel et al.**[5] observed that the turbulent boundary layer thickens very rapidly and is accompanied by (a) significant variation in static pressure across the boundary layer, and (b) a dramatic decrease in the Reynolds stress. They concluded that

> (i) the static pressure variation across the layer implies an interaction between the turbulent rotational flow in the boundary layer and the potential flow outside and that prediction of these flows cannot be separated but must be done simultaneously, and

> (ii) in order to calculate the development of a thick turbulent boundary layer it is necessary to include not only the direct effects of pressure but also the indirect effect of transverse curvature on the turbulence as reflected in the decrease in mixing length and eddy-viscosity.

Cebeci[6] developed an eddy viscosity formulation for the thick turbulent boundary layer. The model was based on experimental measurements and an empirical "law of the wall" for flows over thin cylinders and is appropriate to external flows only.

While the literature is replete with studies of transverse curvature effects in external flows it is equally sparse in studies of internal flows. **Patel[7]** considered an integral method for the calculation of thick axisymmetric boundary layers and included an internal flow case. (The flow in a conical diffuser was considered; transverse curvature effects were isolated as there was no longitudinal curvature.) Patel's method (an extension of the von Kármán integral method for flows with lateral pressure gradients) worked well for external flows but was unsuccessful at predicting the internal flow boundary layer development. He attributed this to the influence of turbulent terms which were omitted from the momentum integral equation. Physically, just as the Reynolds stress had diminished in the external flow, Patel expected a corrresponding <u>increase</u> in the turbulence level due to transverse curvature in internal flows.

The effects of transverse curvature have been discussed frequently in the literature but there isn't much discussion of exactly under what conditions the phenomenon becomes important. Generally speaking, most authors state that when the thickness of the boundary-layer on a body of revolution becomes of the same order as the local radius of the body, the influence of transverse (or lateral) curvature becomes appreciable.

Some specific data have been reported in the literature, however. **Patel et al.[5]** observed in their experiments at the aft end of a body of revolution that

- static pressure remains substantially constant through the boundary-layer right up to x/L = 0.90. For x/L > 0.90 the static pressure decreases from the wall towards the edge of the boundary-layer.

- up to x/L = 0.90 the normal component of the velocity is small compared with the longitudinal component as required by thin boundary-layer theory. By x/L = 0.99, however, the normal component of velocity is almost 32% of the longitudinal component at the edge of the boundary-layer.

- the streamlines are convex and nearly parallel to the surface inthe region x/L < 0.90 where the boundary-layer is thin, and concave and divergent over the last 10% of the body length.

Fortunately, **Patel et al.**[5] measured the boundary-layer thickness over the length of the body. They found that the change from thin to thick boundary-layer behavior takes place in the region of $x/L = 0.90$ where δ/r_0 is approximately 0.62 (r_0 is the body radius).

In another paper, **Patel**[7] reports on other experiments (not his own) where the boundary-layer thickness is thin compared with the body radius (up to $x/L = 0.70$ (where $\delta/r_0 < 0.115$) and beyond $x/L > 0.7$ the boundary-layer cannot be regarded as thin. These data are quite different from the ones reported above and so the results are inconclusive. The difference may be attributable to different body shapes and consequently different free-stream velocity distribution along the bodies.

The above-mentioned experiments were conducted with incompressible fluids. We haven't been able to identify any comparable data for experiments with compressible fluids. However, **White et al.**[8] reported on experiments in supersonic flows over slender cylinders and cones. Their results show that the skin friction coefficient is very sensitive to the transverse Reynolds number ($R_a = U_\infty r_0 / \nu_e$; r_0 = body radius) for flow over a slender cylinder (C_f increases by up to 100% for $R_a = 100$ over flat plate values [$R_a = \infty$]). Slender cones in supersonic flow were similarly shown to have higher skin friction than would be predicted by flat plate (thin boundary-layer) theory.

The above discussion has been limited to boundary-layers in external flows, which have received much more attention the literature than internal flows with thick boundary-layers. Nevertheless, **Whitfield and Lewis**[9] reported results from experiments on _laminar_ boundary-layer development in nozzles. In their experiments the boundary-layer thickness was as high as 90% of the nozzle radius. The effects of transverse curvature on the boundary-layer thickness were reported to be as large as 15%. These effects should be accounted for in the BLM program [3] which already includes the effects of transverse curvature in the mean flow.

3. Longitudinal Curvature Effects

Longitudinal curvature can affect boundary-layer structure through the influence of centrifugal force and/or normal stresses when the streamlines are curved. **Cebeci & Bradshaw**[4] discuss the mean flow terms and their order of magnitude relative to the other boundary-layer terms. They point out that centrifugal force terms are generally intractable and normal stresses are usually negligible in weakly turbulent flows. For this reason the thin boundary-layer approach is usually adopted even in cases where it isn't strictly applicable. Moreover, they claim that attempts to approximate, rather than neglect, $\partial p/\partial y$ changes the equation type back to elliptic, and methods of solution intended for parabolic equations may not work. They do not elaborate on this nor do they discuss boundary conditions for these flows.

Normal stresses have received relatively little attention in the literature. **Finley**[10] analyzed experimental data from cooled-wall and adiabatic hypersonic flow nozzles. He attributed the large variation of static pressure in hypersonic nozzle boundary-layer flows to be the combined effects of longitudinal curvature of the mean streamlines and the increasing importance, as the Mach number rises, of the Reynolds stress contribution to the total normal stress perpendicular to the wall. He concluded that at its peak value the Reynolds stress may provide a normal stress contribution equal to that of the mean static pressure.

The influence of longitudinal curvature on the mean boundary-layer flow can be modeled in several ways. The first way, pointed out by many authors, is to simply include the centrifugal force term in the y-momentum equation, to wit

$$\frac{\partial p}{\partial y} \approx \rho u \frac{\partial v}{\partial x} \approx \frac{\rho u^2}{R_0}$$

where R_0 is the longitudinal radius of curvature of the body. **Cebeci and Bradshaw**[4] point out that the usual assumption (that $\partial p/\partial y$ is of the order of o/L times the order of $\partial p/\partial x$) is <u>not</u> because δ/L is small but that the surface is flat. The above equation is derived on the premise that flat-surface terms are small compared to the "centrifugal term" which is justified if $L/R_0 \gg \delta/L$.

Although this was derived from an order of magnitude analysis it isn't very satisfying becasue the probelm of longitudinal curvature is not really addressed, that is, its influence may go deeper than just the one term. Indeed, that is what more thorough analyses have shown.

Two rigorous approaches to modeling the effects of longitudinal curvature (on the mean flow) have been taken in the literature. These are the singular perturbation analysis of **Van Dyke**[11, 12] and the metric influence of curvature method of **Schultz-Grunow and Breuer**[13].

The singular perturbation theory is too complex to go into here. Suffice it to say that starting with the Navier-Stokes equations the problem is solved by a scheme of successive approximations by the method of inner and outer expansions. Two complementary expansions are constructed simultaneously, and matched in their overlap region of common validity. To lowest order in the inner region the Prandtl boundary-layer theory is recovered while the outer region is an inviscid flow. Higher-order solutions in each region give the perturbations to the boundary-layer and external flows. For example, the boundary-layer displacement effect shows up in both the inner and outer regions. The perturbation method simpifies the problem because viscous effects are confined to the inner region which is parabolic and hence easier to solve than the full (elliptic) Navier-Stokes equations.

An important point about the perturbation methods is that higher-order equations are linear, even though the lowest-order equations may be non-linear. This is readily seen in the first- and second-order inner region (boundary-layer) equations for incompressible, laminar flow. In terms of the stream function and body coordinates (x,y) (see **Van Dyke**[11] for details)

first-order:

$$\psi_{1yyy} + \psi_{1x}\psi_{1yy} - \psi_{1y}\psi_{1xy} = -\Psi_{1Y}(x,0)\,\Psi_{1xY}(x,0)$$

second-order:

$$\psi_{2yyy} + \psi_{1x}\psi_{2yy} + \psi_{1yy}\psi_{2x} - \psi_{1y}\psi_{2xy} - \psi_{1xy}\psi_{2y} = \text{inhomogeneous terms}$$

where the right-hand-side of the first-order equation is the longitudinal pressure gradient terms arising from the first-order outer solution. The "inhomogeneous terms" in the second-order equation include the effects of longitudinal curvature, transverse curvature, displacement of the outer flow, and external vorticity. The important point is that all these inhomogeneous terms depend only upon the known first-order solutions.

The boundary conditions (in addition to the free stream condition and no-slip condition) are all formally derived in the matching procedure and pose no probelms. The method of matched asymptotic expansions is limited only by what can be classified as a perturbation and the number of terms required for asymptotic convergence. (Some asymptotic series are actually divergent, a point is reached beyond which additional terms increase the error. Nevertheless, this does not compromise the validity of the expansion, it merely limits it to smaller values of the expansion parameter.)

The approach of **Schultz-Grunow and Breuer**[13] is considerably different from the perturbation approach. They adopt a curvilinear system of coordinates and take the arc length along the surface as the x-coordinate. This brings the longitudinal curvature directly into the problem (since any differntiation with respect to x carries a factor of the ratio of curvature radii [wall position to actual position]). **Schultz-Grunow and Breuer** derive the boundary-layer equations from an order of magnitude analysis performed on the complete Navier-Stokes equations. They obtain the following set of equations:

Continuity:
$$\frac{\partial u}{\partial x} + \frac{\partial}{\partial y}(1+ky)v = 0$$

x-Momentum:
$$u\frac{\partial u}{\partial x} + (1+ky)v\frac{\partial u}{\partial y} + kuv = -\frac{1}{\rho}\frac{\partial p}{\partial x} + (1+ky)\nu\frac{\partial^2 u}{\partial y^2} + \nu k\left[\frac{\partial u}{\partial y} - \frac{ku}{1+ky}\right]$$

y-Momentum:
$$ku^2 = \frac{1+ky}{\rho}\frac{\partial p}{\partial y}$$

where $k = 1/R_0$. These equations are valid for concave as well as convex surfaces ($y > 0$ for convex walls and $y < 0$ for concave walls).

The authors point out that these equations contain all the second-order terms of the second-order perturbation theory (Van Dyke[11]), namely those of order $1/\sqrt{Re}$, and the exact metric influence of curvature. An additional term was included in the equations as well (the only justification given is that the main flow is then an analytic solution of the boundary-layer equations [sic]). Also note that these equations reduce to the classical boundary-layer equations when $k = 0$.

Longitudinal curvature has an effect on the structure of turbulence as well. In a boundary layer on a convex wall the centrifugal forces exert a small stabilizing effect. In contrast with that, concave walls have a de-stabilizing effect due to instabilites known as Taylor-Görtler vortices. Physically, the fluid element in a curved stream whose angular momentum decreases with increasing distance from the center of curvature is unstable. If the element is slightly displaced outward from the center, conserving its angular momentum about the center, it will be moving faster than its surroundings (which have a smaller angular momentum). Therefore the radial pressure gradient that controls streamline curvature will be too small to direct the displaced element along a streamline of the main flow, and the element will move even further outward. The converse argument holds for inward displacement. These instabilities affect both the transition to turbulence and the eddy viscosity. Bradshaw[14] developed an expression for the effect of longitudinal curvature on eddy-viscosity based on an analogy between streamline curvature and buoyancy in turbulent shear flows (more on this later).

Cebeci, Hirsch, & Whitelaw[15] analyzed the turbulent boundary layer on a (convex) longitudinally curved surface using the mean flow equations of Schultz-Grunow and Breuer[13] discussed above. In their treatment they replaced the laminar viscosity with an effective viscosity, $\nu + \epsilon_m$. The eddy viscosity (ϵ_m) was specified to be the standard Cebeci and Smith[16] eddy-viscosity formulation modified by Bradshaw's[14] correction for longitudinal curvature.

Cebeci and Smith[16] point out that streamline curvature may increase or decrease the turbulent mixing, depending on the degree of wall curvature, and it can strongly affect the skin friction and heat transfer coefficients. They also indicate how the streamwise curvature can be incorporated into the eddy-viscosity exrpession by multiplying the right-hand-side of the inner eddy-viscosity expression by S^2 (**Bradshaw's**[15] correction), where

$$S = \frac{1}{1 + \beta Ri}, \qquad Ri = \frac{2u}{R_0}\left(\frac{\partial u}{\partial y}\right)^{-1}$$

where Ri is analogous to the Richardson number and R_0 is the longitudinal radius of curvature. (See the next section for additional discussion of the Richardson number.) The parameter β is equal to 7 for convex surfaces and 4 for concave surfaces, according to meteorological data and by **Bradshaw's**[14] analogy between streamline curvature and buoyancy. Accordig to Bradshaw, the effects of curvature on the mixing length or eddy-viscosity are appreciable if the ratio of boundary-layer thickness to radius of curvature, $\delta : R$, exceeds roughly $1 : 300$.

We will complete this discussion of **Cebeci et al.**[15] by citing the boundary conditions used in their paper:

$$@\ y = 0:\ u = v = 0; \qquad @\ y = \delta:\ u_e = \frac{u_w(x)}{(1 + ky)}$$

where the condition at $y = 0$ was obtained assuming $v = 0$ and vanishing vorticity in the free stream and $u_w(x)$ is the inviscid velocity distribution.

4. Fluid Stratification Effects

Fluid stratification (i.e., density gradients) can be of importance in the presence of longitudinal curvature. However, the manifestation of density gradient effects is sufficiently different that it is discussed separately here.

The influence of fluid stratification is limited to the eddy-viscosity inasmuch as the centrifugal force terms are explicitly included in the mean flow equations. In compressible, turbulent flows there is a coupling of the density and velocity fluctuations which leads to Reynolds stress-type terms. Physically, the turbulence is affected by the interaction of the density gradient and centrifugal forces. This interaction can enhance or diminish the turbulent mixing depending on the sense of the density gradient. In the extreme case, a turbulent flow can be laminarized by centrifugal forces. That is, in a stably stratified fluid turbulent mixing is suppressed by the restoring force of the pseudo-buoyancy. Conversely, if the fluid is unstably stratified, the turbulent mixing is enhanced by the centrifugal force.

Fluid stratification effects are usually discussed in meteorological applications where it is more aptly described in terms of buoyancy forces (rather than centrifugal forces). The dimensionless variable usually used to describe the influence of buoyancy is the gradient Richardson number (see, for example, Turner[17])

$$Ri = \frac{-g \frac{\partial \rho}{\partial z}}{\rho \left(\frac{\partial u}{\partial z}\right)^2}$$

which is the ratio of buoyancy force to shear stress force; g is the gravitational acceleration and z is the altitude. This dimensionless parameter is readily modified for flows with centrifugal forces by substituting the centrifugal acceleration for the gravitational acceleration. Thus we might say

$$Ri^* = \frac{\dfrac{u^2}{R_0}\dfrac{\partial \rho}{\partial y}}{\rho\left(\dfrac{\partial u}{\partial y}\right)^2}$$

is a modified Richardson number for boundary-layer flow with longitudinal curvature. Physically, the centrifugal force would suppress the turbulence on a cold, concave surface.

Observations of fluid stratifiaction effects have been made mostly in combustion devices where there are (a) large density gradients and (b) strong swirling flows (with centrifugal accelerations exceeding 25,000 g's). Accordingly, most of the analyses we are familiar with have been numerical solutions of elliptic flows. We have not found any reference to fluid stratification effects on longitudinally curved boundary layers. However, Bradshaw[14] does point out that curvature effects on skin friction and heat transfer can be much larger at high supersonic speeds.

5. Recommendations

OTV nozzles exhibit all the effects discussed above, though it is hard to say which of them might dominate. We haven't found anything in the literature to account for the increase in turbulent mixing due to transverse curvature in internal flows. We have no recommendation to make here except perhaps to pursue further literature searching. Likewise, we have found no discussion of fluid stratification effects. We recommend calculation of the modified Richardson number given in the previous section and comparison with Bradshaw's Richardson-like number given in Section 3. This may shed some light on the relative importance of longitudinal curvature and density gradient effects.

Most likely the strongest influence on the boundary layer comes from the longitudinal curvature effect on the lateral pressure distribution in the boundary layer. Fortunatley, these effects have been treated adequately in the literature. We recommend application of **Schultz-Grunow and Breuer's**[13] formulation for the mean flow equations in conjunction with the **Cebeci and Smith**[3, 10] eddy-viscosity model and **Bradshaw's**[14] correction for longitudinal curvature. These models are appropriate to both convex and concave surfaces. Furthermore, they have been successfully applied to turbulent boundary layer calculations in (convex) longitudinally curved surfaces by **Cebeci et al.**[15]. Finally, these formulations should be compatible with the current BLM program (**Cebeci**[3]) in use at Software & Engineering Associates, Inc. and can probably be incorporated into the program withonly a moderate effort.

6. References

1.   **BLIMP-J** User's Manual, prepared by M. Evans, Aerotherm Division/Acurex Corporation, July 1975 under Contract NAS8-30930.

2.   **Weingold, H. D.,** "The ICRPG Turbulent Boundary Layer (TBL) Reference Program," prepared for ICRPG Performance Standards Working Group, July 1968.

3.   **Cebeci, T.,** "Boundary Layer Analysis Module," prepared for Software & Engineering Associates, Inc., January 1982.

4.   **Cebeci, T. and Bradshaw, P.,** Momentum Transfer in Boundary Layers, McGraw-Hill, New York, 1977.

5.   **Patel, V. C., Nakayama, A., and Damian, R.,** "Measurements in the thick axisymmetric turbulent boundary layer near the tail of a body of revolution," J. Fluid Mech., Vol. 63, Part 2, pp.345-367, 1974.

6.   **Cebeci, T.,** "Eddy-Viscosity Distribution in Thick Axisymmetric Turbulent Boundary Layers," J. Fluids Engrg., Transactions of the ASME, Vol. 95, Ser. I, No. 2, pp. 319-326, June 1973.

7.   **Patel, V. C.,** "A Simple Integral Method for the Calculation of Thick Axisymmetric Turbulent Boundary Layers," Aeronautical Quarterly, Vol. 25, Part 1, pp. 47-58, February 1974.

8.   **White, F.M., Lessman, R.C., and Christoph, G.H.,** "Analysis of Turbulent Skin Friction in Thick Axisymmetric Boundary Layers," AIAA J., Vol. 11, No. 6, pp. 821-825, June 1973.

9.   **Whitfield, D.L. and Lewis, C.H.,** "Boundary Layer Analysis of Low-Density Nozzles, Including Displacement, Slip, and Transverse Curvature," J. Spacecraft and Rockets, Vol. 7, No. 4, pp.462-468, April 1970.

10. **Finley, P. J.,** "Static Pressure in Hypersonic Nozzle Boundary Layers," AIAA J., Vol. 15, No. 6, pp. 878-881, June 1977.

11. **Van Dyke, M.,** "Higher approximations in boundary-layer theory, Part 1. General analysis," J. Fluid Mech., Vol. 14, Part 1, pp. 161-177, 1962.

12. **Van Dyke, M.,** Perturbation Methods in Fluid Mechanics, Academic Press, 1964.

13. **Schultz-Grunow, F. and Breuer, W.,** "Laminar Boundary Layers on Cambered Walls," in Basic Developments in Fluid Mechanics, Vol. 1, Academic Press, New York, 1965.

14. **Bradshaw, P.,** "The analogy between streamline curvature and buoyancy in turbulent shear flow," J. Fluid Mech., Vol. 36, Part 1, pp. 177-191, 1969.

15. **Cebeci, T., Hirsch, R. S., and Whitelaw, J. H.,** "On the Calculation of Laminar and Turbulent   Boundary Layers on Longitudinally Curved Surfaces," AIAA J., Vol. 17, No. 4, pp. 434-436, April 1979.

16. **Cebeci, T. and Smith, A. M. O.,** Analysis of Turbulent Boundary Layers, Academic Press, New York, 1974.

17. **Turner, J.S.,** Buoyancy Effects in Fluids, Cambridge University Press, 1973.

21 May 1984

MULTIPLE SHOCK WAVE
CONSTRUCTION WITH TDK

Method of Approach

The logic for shock tracing methods becomes highly complex when two or more shocks are to be traced. However, shock tracing methods must be used in order to achieve the numerical accuracy required for nozzle performance prediction. Four work tasks are proposed below that will give the TDK program a capability of dealing with more than one shock wave.

Task 1) Start the MOC calculation with a LRC construction.

The effect of this construction is to ignore the shock originating from the tangent point on the attachment circle. The present method of RRC construction that ignores the first shock by terminating intersecting RRC's can lead to erroneous results. The LRC option would be useful when one wants to ignore the tangent point shock and evaluate the effect of a shock downstream of the attachment point.

The task consists of implementing the construction logic and making it compatible with all the existing options.

Task 2) Make the RRC construction more reliable.

The present MOC initial line is more suitable for LRC than it is for RRC construction. However, if the shock originating from the attachment point is to be traced, one has to start with a RRC construction.

This task consists of investigating the stability of the RRC calculation when starting from the initial line and making the appropriate changes to have a reliable calculation.

Task 3) Allow discontinuous slope in wall contour.

This task will allow a wall contour to be input with a discontinuous slope at one point. This option will be very useful when an attached shock is to be analyzed.
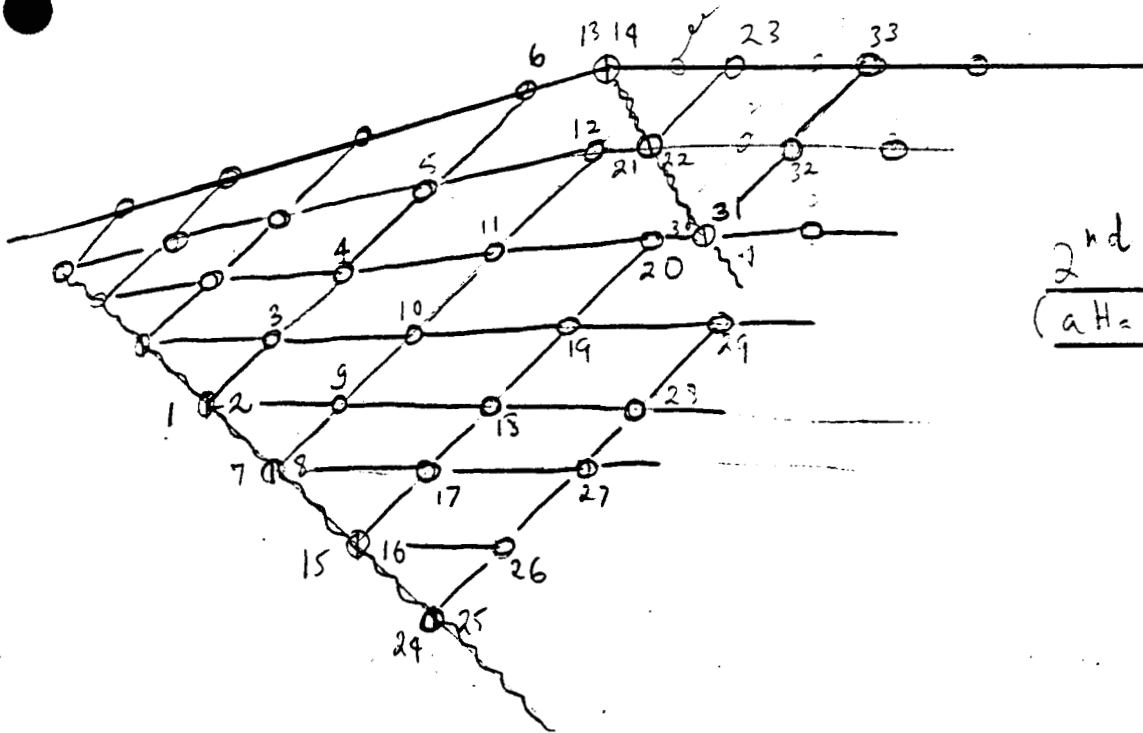
Task 4)   <u>Trace two right-running shocks (RRS)</u>.

This task consists of tracing two RRS's where the first RRS is induced and the second RRS is an attached shock. The intersection of the two RRS's is allowed and may be traced to the axis, but the reflected shock will not be treated. Details of the intersection of two shocks (RRS - RRS) and (RRS - LRS), and of the MOC construction of tracing two RRS, are attached.
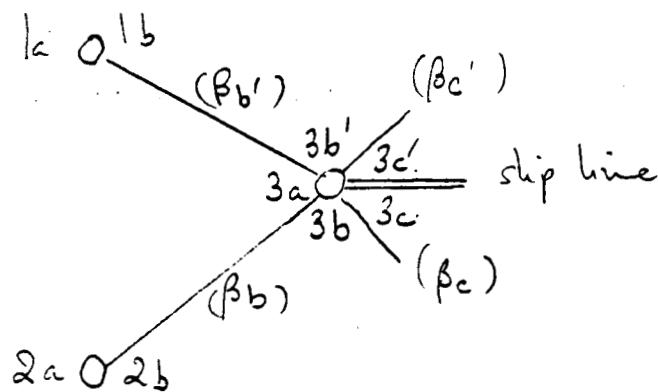
MOC construction for two RRS

2nd shock
(attached)

1st shock
(induced)

SUBROUTINE RSLS

This subroutine calculates the intersection of a right-running and a left-running shock Points $3a, 3b, 3b', 3c, 3c'$ are calculated using the known points $1a, 1b, 2c, 2b$ as shown in the figure below.

The procedure used consists of 3 steps, as follows:

1) Points $3a, 3b$ are calculated from $2a, 2b$ as a LRS, using subroutine SHCKL

2) The shock angle at $1a, 1b$ is used to obtain properties at $3b'$ from $3a$. The same procedure applies to $3b$

3) The shock angles $\beta_{c'}$ and β_c are adjusted so that

$$\theta_{3c} = \theta_{3c'}$$

$$P_{3c} = P_{3c'}.$$

A slip line may exit at $3c, 3c'$ since T, V, ρ may not the same at $3c$ and $3c'$.

Details of step 3) are given below.

● 0) Set $\beta_{c'} = \beta_b$ initially

1) Using $\beta_{c'}$, calculate properties at $3c'$.

2) Set $\theta_{3c} = \theta_{3c'}$. Using subroutine SHOCK, iterate
for the shock angle β_c that gives the deflection $\delta_{3c} = \theta_{3c} - \theta_{3b}$
The properties at $3c$ are obtained at the same time.

3) Set $P_{3c'} = P_{3c}$. Using subroutine SHOCK, iterate for
a shock angle β such that $P_{3c'}$ is equal to the
pressure obtained from $P_{3b'}$ across the shock.

 Set $\beta_{c'} = (\beta_{c'} + \beta)/2$ and go to step 1)

● 4) iterate step 1-3 until convergence in $\beta_{c'}$.

●

SUBROUTINE RSRS

This subroutine calculates the intersection of two right-running shocks. Points $3b, 3b''$ are calculated using the known points $1a, 1b, 2a, 2b$, as shown in the figure below.
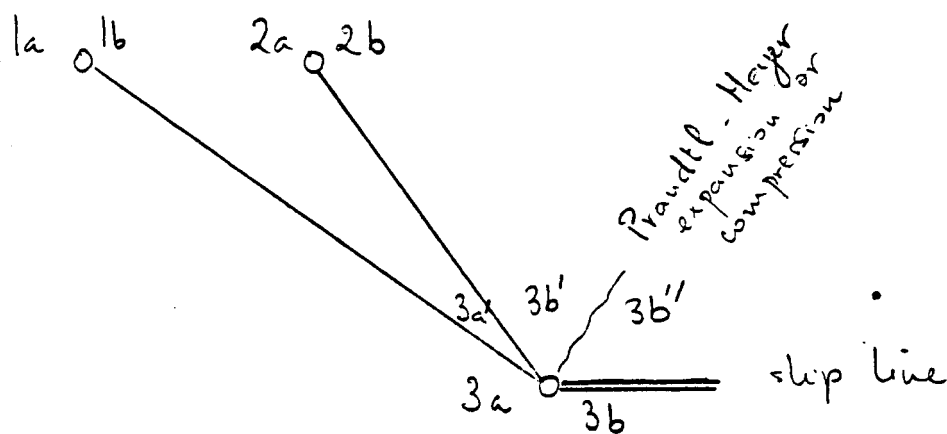
The procedure used consists of 3 steps, as follows:

1) Points $3a, 3a'$ are calculated from $1a, 1b$ as a RRS point, using subroutine SHCKR

2) The shock angle at $2a, 2b$ is used at $3a'$ to obtain properties at $3b'$

3) The shock angle at $3a, 3b$ and the Prandtl-Meyer turning angle are adjusted so that

$$\vartheta_{3b''} = \vartheta_{3b}$$

$$P_{3b''} = P_{3b}.$$

A slip line may exist at $3b, 3b'$ since T, V, ρ may not be the same at $3b$ and $3b''$

Details of step 3) are given below

ORIGINAL PAGE IS
OF POOR QUALITY

● 0) Set $\theta_{3b}'' = \theta_{3b}'$ initially

1) Using the basic SHOCK subroutine, iterate for a shock angle β_3 (at $3a, 3b$) such that the deflection angle is $\delta_3 = \theta_{3b}'' - \theta_{3a}$. The conditions at $3b$ are obtained at the same time.

2) Using the isentropic relation

$$\frac{\left(1 + \frac{\gamma+1}{2} M_{3b}^2\right)^{\frac{\gamma}{\gamma-1}}}{\left(1 + \frac{\gamma+1}{2} M_{3b''}^2\right)^{\frac{\gamma}{\gamma-1}}} = \frac{P_{3b}''}{P_{3b}'} \quad , \quad \text{with } P_{3b}'' = P_{3b}$$

$$M_{3b''} = \sqrt{\frac{q^{\frac{\gamma-1}{2}} - 1}{\frac{\gamma+1}{2}}} \quad , \quad q = \frac{\left(1 + \frac{\gamma+1}{2} M_{3b'}^2\right)^{\frac{\gamma}{\gamma-1}}}{\frac{P_{3b}''}{P_{3b}'}}$$

3) the flow angle at $3b''$, θ_{3b}'', is calculated from the Prandtl-Meyer function, $\nu(M)$,

$$\theta_{3b}'' = \theta_{3b}' + \nu(M_{3b'}) - \nu(M_{3b''})$$

4) Go back to step 1) and iterate until convergence. The conditions at $3b$ are obtained from the shock angle, β_3 and point $3a$. The conditions at $3b''$ are obtained from $3b'$ using the isentropic relations. Aside from θ and P, the other properties at $3b''$ and $3b$ may not be the same, therefore creating a slip line.